

# The association between the configuration of tricuspid annular plane systolic excursion and right atrial contractile strain

Sena Sert, Lale Dinç Asarcıklı, Mehmet Fatih Yılmaz, Levent Pay, Ayca Esen Zencirci, Aysel Yağmur, Barış Güngör, Özlem Yıldırım Türk

Department of Cardiology, Dr. Siyami Ersek Thoracic and Cardiovascular Surgery Training and Research Hospital, Istanbul, Turkey

## Correspondence to:

Sert Sena, MD,  
Department of Cardiology,  
Dr. Siyami Ersek Thoracic and  
Cardiovascular Surgery Training  
and Research Hospital,  
13 Tıbbiye Cad., Selimiye,  
34668, Uskudar, Istanbul, Turkey,  
phone: +90 532 350 84 50,  
e-mail: senasert@live.com

Copyright by the Author(s), 2023  
DOI: 10.33963/KPa2022.0273

## Received:

August 15, 2022

## Accepted:

November 24, 2022

## Early publication date:

November 30, 2022

## ABSTRACT

**Background:** In the descending arm of tricuspid annular plane systolic excursion (TAPSE), there is notch formation that corresponds to the contractile phase of the atrial strain curve. Theoretically, this notch formation stands for atrial contraction.

**Aims:** We aim to characterize notch formation on TAPSE, predictors of its existence, and its relationship with the right ventricle and right atrial strain (RAS) parameters.

**Methods:** Retrospectively selected 240 patients were investigated for the determinants of notch formation on TAPSE and the relationship between RAS and TAPSE. RAS was analyzed using 2D speckle tracking in a dedicated mode for atrial analysis and reported separately for the reservoir, conduit, and contractile phases.

**Results:** 71.7% (n = 172) of patients had notch formation on TAPSE and 70.4% (n = 169) had a normal value of right atrial contractile strain (RAS<sub>ct</sub>). Most patients with notch formation also had preserved RAS<sub>ct</sub> (95.9%; P < 0.001). In multivariable analysis, RAS<sub>ct</sub> (odds ratio [OR], 1.45; 95% confidence interval [CI]: 1.13–1.77; P = 0.020) remained significant with notch formation. Receiver operator characteristic (ROC) analysis demonstrated that a RAS<sub>ct</sub> of –19% was a cut-off for the presence of notch formation. ROC area was 0.897 (95% CI 0.844–0.951; P < 0.001).

**Conclusions:** The changes in TAPSE configuration reflect the changes in the atrial contractile phase. The descending arm of TAPSE indicates RAS<sub>ct</sub> as to whether it is preserved or not. Notch formation persists if RAS<sub>ct</sub> is above –19%. So, an easier, more applicable, and more effortless tool, TAPSE, can be used as an indicator of the atrial contractile phase by its configuration in daily routine.

**Key words:** atrial contractile strain, right atrial strain, tricuspid annular plane systolic excursion

## INTRODUCTION

In recent years, a growing number of studies have focused on the data investigating the right atrium (RA), its mechanics, and normal reference values of its diameter, area, and other metric values and functions. After recognition of the diagnostic and prognostic impact of the RA on different cardiovascular diseases, such as pulmonary embolism, pulmonary hypertension (PH), and heart failure (HF), its role during the cardiac phases has also been explored [1–4].

Formerly, the atrial cavities were ascribed the minimalistic role of “transit chambers”,

but the atria serve three distinct functions during the cardiac cycle. The RA works as a reservoir during ventricular systole against the closed tricuspid valve, and after opening of the tricuspid valve, it serves as a passive conduit during early diastole. Finally, it has a booster pump role during atrial contraction in late diastole until the tricuspid valve closes [5, 6]. All of these phases are modulated by loading conditions, heart rate, and intrinsic contractility of the atria [7]. Concerning right atrial strain (RAS), the American Society of Echocardiography (ASE) and the European Association of Cardiovascular Imaging (EACVI)

## WHAT'S NEW?

The changes in the configuration of the tricuspid annular plane systolic excursion (TAPSE) curve reflect the changes in the atrial contractile phase. If right atrial contractile strain ( $RAS_{ct}$ ) is above  $-19\%$ , we observed that there was a notch that corresponds to late diastole during the atrial contraction in the descending arm of TAPSE. So, this notch formation of the TAPSE curve indicates whether the  $RAS_{ct}$  phase is preserved or not. TAPSE and right atrial strain have similar courses when  $RAS_{ct}$  remains preserved. Therefore, instead of right atrial strain analysis, which is a cutting-edge technique, TAPSE can be an indicator of the atrial contractile phase as an easier and more available tool. We suggest that TAPSE curve configuration can be used to estimate  $RAS_{ct}$  in daily practice.

have published a consensus document addressing standards for two-dimensional (2D) speckle tracking echocardiography (STE) of the RA that is a useful non-invasive tool for assessment of atrial function [8].

On the other hand, tricuspid annular plane systolic excursion (TAPSE) is the traction of the lateral annulus of the tricuspid valve toward the apex during ventricular systole. The incline of TAPSE reflects the traction of the right ventricular (RV) lateral wall during ventricular systole-RV contractility in the long axis, and it corresponds to atrial diastole in which the RA works as a reservoir, which is also called the atrial reservoir phase. The first part of the

descending arm of the TAPSE curve represents the passive part — the conduit phase in the early ventricular diastole and the second part of TAPSE decline represents the atrial booster phase in the late ventricular diastole [9].

When atrial strain curves are examined, it is easy to realize their resemblance to the TAPSE curve. The TAPSE curve shows the formation of a notch in the descending arm while the atrial strain curve shows the contractile phase when atrial contraction occurs (Figure 1). Theoretically, this notch formation in the TAPSE curve stands for atrial contraction. But somehow in our daily practice, it has been observed that some patients have a smooth formation in

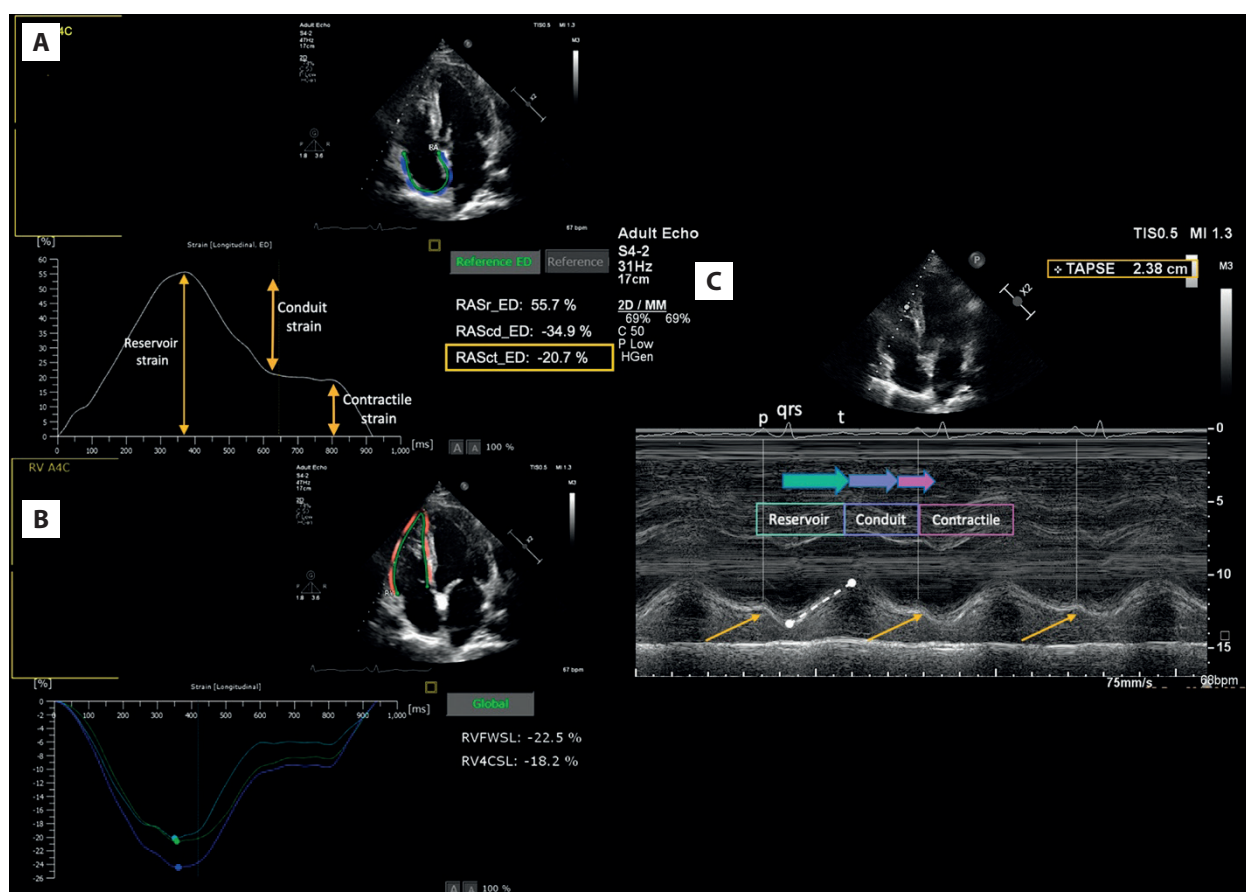


**Figure 1.** Similarity between atrial strain curve and TAPSE configuration and notch formation in the TAPSE curve while right atrial contractile strain is preserved. **A.** Right atrial strain curve. **B.** Right ventricular strain curves. **C.** TAPSE analyses and notch formation in the descending arm

Abbreviations:  $RA_{sr\_ED}$ , end-diastolic right atrial reservoir strain;  $RAS_{cd\_ED}$ , end-diastolic right atrial conduit strain;  $RAS_{ct\_ED}$ , end-diastolic right atrial contractile strain; RVFWS, right ventricular free wall strain; RVGLS, right ventricular global longitudinal strain; TAPSE, tricuspid annular plane systolic excursion

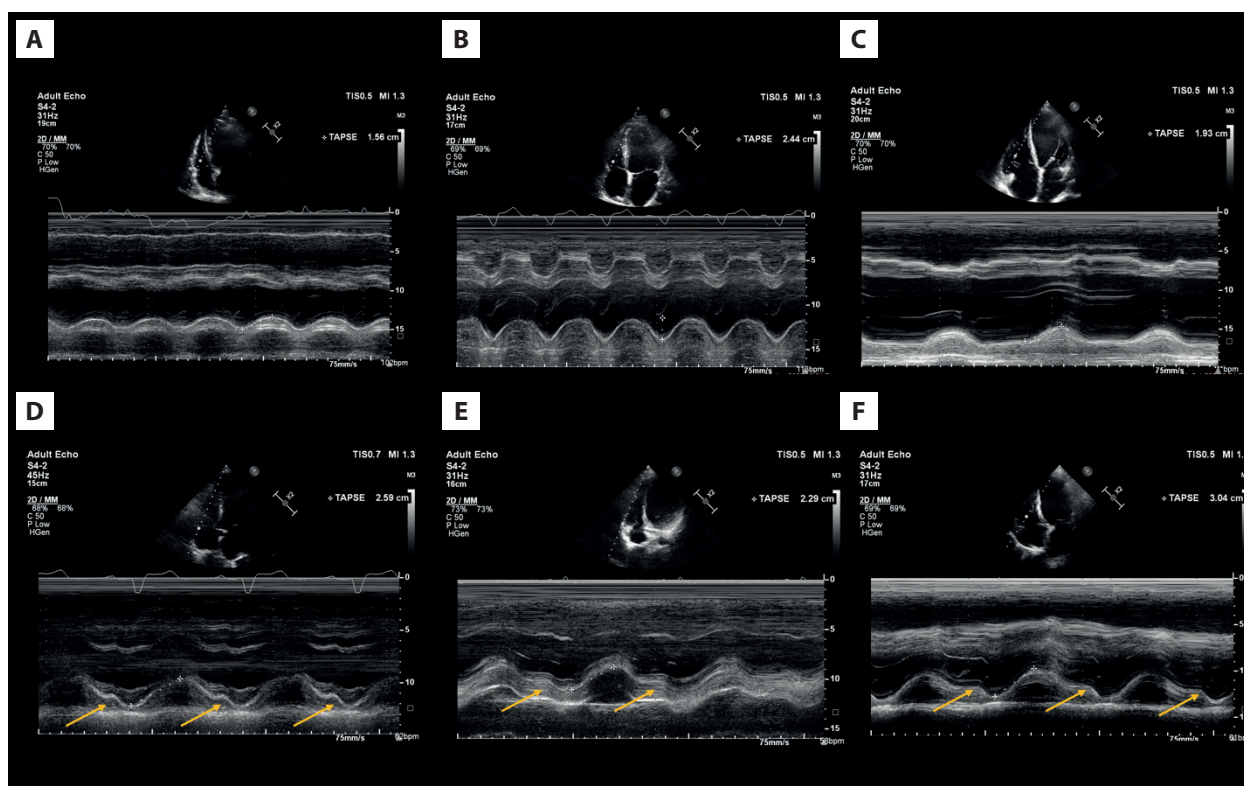


**Figure 2.** **A, B,** and **C.** TAPSE curves without notch formation. **D, E,** and **F.** Notch formation at the late diastole simultaneously with the P wave (arrows). **A.** Right atrial strain curve. **B.** Right ventricular strain curves. **C.** TAPSE analyses and notch formation in the descending arm  
Abbreviations: see [Figure 1](#)

the descending arm while others have a notch on it ([Figure 2](#)). Currently, there is a paucity of data on the impact of notch formation on TAPSE and the interrelation between TAPSE and RAS. In this study, we aimed to characterize notch formation in the TAPSE curve, its predictors, and its relationship with the RV and RA strain patterns.

## METHODS

### Study population

We retrospectively selected 290 patients with sinus rhythm without previous cardiac surgery. Between March 2021 and March 2022, we enrolled all subjects who were referred to our Echocardiography Laboratory for examination due to routine follow-up of underlying stable coronary artery disease, compensated and clinically stable heart failure, hypertension, diabetes, hyperlipidemia, chronic kidney disease, as well as healthy individuals to be investigated for possible cardiac pathology. Since we had planned to investigate the determinants of notch formation on TAPSE and the relationship between RAS and TAPSE, a sample with a wide range of patients was created to investigate the effect of different pathologies on the outcome. We considered it important to include a wide range of different cardiac disorders to better examine possible differences between different scenarios. However, patients with one or more of the following “specific cardiovascular diseases”

were excluded: atrial fibrillation, primary pulmonary hypertension, severe tricuspid regurgitation and/or stenosis, pericardial diseases, restrictive or hypertrophic cardiomyopathies, or paced rhythms. Fifty patients were excluded from the study because they were difficult to assess due to poor imaging quality and frequent extrasystoles.

### Echocardiography

Echocardiography was performed using an EPIQ ultrasound system equipped with a matrix-array S-4 transducer (Philips Medical Systems, Andover, MA, US) by a single experienced sonographer. All images were recorded between 08:00–10:00 am with an empty stomach after at least 6 hours of fasting to provide standardization in volume status. Care was taken so that the images include the entire RV. TAPSE, systolic excursion velocity (RV S'), and right ventricular global longitudinal strain (RVGLS) were measured according to the recommendations by the ASE and EACVI [10]. RA strain was analyzed using 2D speckle tracking in a dedicated mode for atrial analysis and reported separately for the reservoir, conduit, and contractile phases as recommended in the EACVI/ASE consensus report [8]. For RAS analyses, we used proprietary software originally designed for the left atrium, and the endocardial border of the RA was manually traced, beginning and ending at the tricuspid annulus, and the width of the region of interest (ROI) was manually adjusted to include the whole

endocardium, but not the pericardium, as recommended. For RV strain analyses, we used proprietary software originally designed for the RV. RASs and RVGLS were measured by speckle tracking echocardiography using frame rates from 40 to 80/s. Measurements were averaged over three cardiac cycles when a patient had sinus rhythm. The time reference used to define the zero baseline for the RAS curves was ventricular end-diastole. The images were digitally stored and analyzed offline (QLab). This analysis was performed using a semiautomatically traced ROI along the RA endocardial border. If necessary, the ROI was adjusted manually. Normative values of RAS were determined by the reference values from the latest multicenter study (WASE Normal Values Study International) that were addressed by EACVI/ASE consensus report on the RA [6, 11].

To test the intra-observer reproducibility of RAS, measurements were repeated two weeks apart in 20 randomly selected patients from the study group. To test the inter-observer reproducibility, the same 20 patients were measured by a second researcher, blinded to the prior measurements. Inter-observer and intra-observer variabilities in each parameter studied were evaluated with an intraclass correlation coefficient (ICC). Inter-observer ICCs of RA reservoir (RAS<sub>r</sub>), conduit (RAS<sub>cd</sub>), and contractile (RAS<sub>ct</sub>) strains were 0.974, 0.877, and 0.910, respectively. Intra-observer ICCs of RAS<sub>r</sub>, RAS<sub>cd</sub>, and RAS<sub>ct</sub> were 0.981, 0.983, and 0.945, respectively.

TAPSE was acquired by using the apical 4-chamber view, the M-mode cursor was placed through the junction of the tricuspid valve plane and RV free wall. TAPSE was determined by the difference in the displacement of the RV base during systole and diastole. The notch on TAPSE was visually assessed and accepted as the hump in the descending arm of the curve.

### Statistical analyses

The numerical variables were investigated using visual (histograms, probability plots) and analytical methods (Kolmogorov-Smirnov/Shapiro-Wilk tests) to determine whether they were normally distributed. Descriptive analyses were presented using mean (standard deviations) for normally distributed variables and medians and interquartile ranges (IQR) for non-normally distributed variables. Categorical variables were compared using the  $\chi^2$  test, which was used to compare the existence of a notch in the descending arm of the TAPSE curve and preserved RAS<sub>ct</sub>. Comparisons between subgroups were performed by using Student's t-test for unpaired data as a parametric test for normally distributed variables and the Mann-Whitney U test as a non-parametric test for non-normally distributed or ordinal variables. The variables affecting each RAS parameter were investigated using Pearson correlations. For multivariable analysis, the possible factors identified with univariable analysis were further entered into the logistic regression analysis to assess which parameters were independent determinants of notch formation in the TAPSE

curve. The area under the receiver operating characteristic (ROC) curve (AUC) was calculated to evaluate the ability of RAS<sub>ct</sub> to estimate notch formation in the TAPSE curve. When a significant cut-off value was observed, sensitivity, specificity, positive, and negative predictive values were presented. A *P*-value <0.05 was considered significant for all the data examined. All statistical analyses were performed using SPSS software Version 22.0 (IBM Corporation, Armonk, NY, US). The study was approved by the Regional Ethics Committees and Institutional Review Boards.

## RESULTS

### Study population and baseline characteristics

Table 1 summarizes the demographic, clinical, and echocardiographic data. The mean (SD) age of the patients was 47 years, and most of the patients were male (75.8%). We observed that 71.7% (*n* = 172) of patients had notch formation in the TAPSE curve and 70.4% (*n* = 169) of patients had a normal value of RAS<sub>ct</sub>. The vast majority of these patients who had TAPSE with notch formation also had preserved RAS<sub>ct</sub> (*n* = 162, 95.9%; *P* < 0.001).

Patients who had TAPSE with notch formation demonstrated a higher RAS<sub>r</sub>, RAS<sub>cd</sub>, RAS<sub>ct</sub>, RVGLS, RV free wall GLS, TAPSE, and RV S'. We noticed that patients who had TAPSE without notch formation had higher heart rates (Table 1). Tachycardia was observed in 35 patients (14.6%) during examination, and we found a significant relationship between tachycardia and the absence of notch formation (Table 1). The frequency of tachycardia among patients who had TAPSE with-notch formation (*n* = 169) was 5.9% (*n* = 10) while it was 35.2% (*n* = 25) for patients who had TAPSE without notch formation (*n* = 71; *P* < 0.001). Age, sex, and the size of right heart chambers did not significantly differ between the two groups. The estimated systolic pulmonary artery pressure (sPAP) was significantly higher in the patients without notch formation.

Univariable logistic regression analysis revealed a significant relationship between notch formation in the TAPSE curve, as well as RAS<sub>r</sub>, RAS<sub>cd</sub>, and RAS<sub>ct</sub> parameters and also RVGLS, RV free wall strain, sPAP, RV S', and TAPSE (Table 2). In the multivariable analysis, RAS<sub>ct</sub> (odds ratio [OR], 1.45; 95% confidence interval [CI], 1.13–1.77; *P* = 0.020), RVGLS (OR, 1.22; 95% CI, 1.09–1.35; *P* = 0.030), and RV free wall strain (OR, 1.20; 95% CI, 1.13–1.27; *P* = 0.026) remained significant with notch formation.

We investigated the correlations between 3 different strain phases of the RA with other echocardiographic values to shed some light on the interaction between these parameters. The results indicated that all 3 phases had a significant correlation with each other and this significant relationship persisted with the RV S', TAPSE, RVGLS, and RV free wall strain (Table 3). We observed that the phase most affected by each RV S', TAPSE, RVGLS, and RV free wall strain was the reservoir phase, followed by the conduit and contractile phases. The results showed that there was

**Table 1.** Demographic and clinical patient characteristics with echocardiographic data

Demographic parameters	All (n = 240)	TAPSE with notch formation (n = 169)	TAPSE without notch formation (n = 71)	P-value
Age, years, mean (SD)	47.4 (11.6)	47.9 (11.5)	46 (11.7)	0.25
Sex, females, n (%)	58 (24.2)	17 (23.9)	41 (24.3)	0.95
BMI, kg/m <sup>2</sup> , mean (SD)	26.3 (3.8)	26.2 (4)	26.4 (3.3)	0.77
Heart rate, beats/min, mean (SD)	80 (17)	76 (15)	90 (17)	<0.001
Tachycardia, n (%)	35 (14.6)	10 (5.9)	25 (35.2)	<0.001
Bundle branch block, n (%)	62 (25.8)	47 (19.5)	15 (6.3)	0.28
Comorbidities, n (%)				
Coronary artery disease	57 (23.7)	20 (8.3)	37 (15.4)	0.05
Diabetes	50 (20.8)	23 (9.6)	27 (11.2)	0.09
Hypertension	81 (33.7)	36 (15)	45 (18.7)	0.06
Chronic renal failure	31 (12.9)	11 (4.6)	20 (8.3)	0.05
Echocardiographic parameters				
Left ventricular end-diastolic diameter, mm, mean (SD)	48.5 (6.9)	48.2 (6.4)	48.6 (6.5)	0.31
Left ventricular end-systolic diameter, mm, mean (SD)	20.4 (4.6)	20.1 (4.3)	20.5 (4.4)	0.26
Left ventricular ejection fraction, %, median (IQR)	55 (40 – 65)	49.9 (40–60)	58 (45–65)	0.24
Estimated systolic pulmonary artery pressure, mm Hg, mean (SD)	29.9 (7.4)	23.9 (8.9)	38.1 (9.9)	<0.001
Tricuspid annular plane systolic excursion, mm, mean (SD)	20.4 (4.9)	21.3 (4.8)	18.3 (4.6)	<0.001
Right ventricular systolic Doppler velocity, cm/sec, mean (SD)	10.9 (3.2)	11.2 (3)	10.1 (3.4)	0.01
Right ventricular basal diameter, mm, mean (SD)	38.5 (6.1)	38.3 (6.1)	39 (6)	0.42
Right atrial area, cm <sup>2</sup> , mean (SD)	16.7 (5.1)	16.7 (5.3)	16.8 (5.4)	0.8
Right ventricular global longitudinal strain, %, mean (SD)	-19.8 (5.2)	-21.3 (4.4)	-16.2 (5.1)	<0.001
Right ventricular free wall strain, %, mean (SD)	-21.7 (6.1)	-23.6 (4.6)	-17.9 (5.3)	<0.001
RA reservoir strain, %, mean (SD)	39.5 (13.6)	44.6 (11.7)	27.2 (8.9)	<0.001
RA conduit strain, %, mean (SD)	-18.2 (6.3)	-20.8 (10.2)	-11.7 (7.3)	<0.001
RA contractile strain, %, mean (SD)	-21.3 (6.7)	-23.6 (5.9)	-15.6 (4.8)	<0.001
Tricuspid inflow E velocity, cm/sec, median (IQR)	0.51 (0.31–0.71)	0.52 (0.32–0.72)	0.5 (0.31–0.69)	0.49
Tricuspid inflow A velocity, cm/sec, mean (SD)	0.74 (0.3)	0.75 (0.3)	0.72 (0.4)	0.59
Tricuspid inflow E/A ratio, mean (SD)	1.15 (0.6)	1.13 (0.6)	1.18 (0.6)	0.62

Abbreviations: BMI, body mass index; RA, right atrium; TAPSE, tricuspid annular plane systolic excursion

**Table 2.** Univariable logistic regression analysis of predictors for notching in the descending arm of the TAPSE curve

Variables	Odds ratio (95% CI)	P-value
RA reservoir strain, %	1.16 (1.12–1.20)	<0.001
RA conduit strain, %	1.11 (1.08–1.14)	<0.001
RA contractile strain, %	1.66 (1.42–1.80)	<0.001
EF, %	1.01 (0.98–1.04)	0.338
RVGLS, %	1.52 (1.26–1.78)	0.001
RV free wall strain, %	1.48 (1.26–1.60)	0.001
sPAP, mm Hg	0.98 (0.97–0.99)	0.026
Right ventricular basal diameter, mm	0.98 (0.93–1.02)	0.424
Right atrial area	0.99 (0.94–1.05)	0.081
RV S'	1.11 (1.01–1.22)	0.020
TAPSE	1.13 (1.06–1.20)	<0.001
Heart rate	0.97 (0.94–0.99)	0.037

Abbreviations: EF, ejection fraction; RA, right atrium; RV, right ventricle; RVGLS, right ventricular global longitudinal strain; RV S', systolic excursion velocity; sPAP, estimated systolic pulmonary artery pressure; TAPSE, tricuspid annular plane systolic excursion

**Table 3.** Relationship between right atrial strain values and other echocardiographic parameters

Variables	RV S'		TAPSE		RVGLS		RVFWS	
	r	P-value	r	P-value	r	P-value	r	P-value
RA-reservoir strain, %	0.570	<0.001	0.653	<0.001	-0.483	<0.001	-0.505	<0.001
RA-conduit strain, %	-0.530	<0.001	-0.591	<0.001	0.397	<0.001	0.427	<0.001
RA-contractile, %	-0.475	<0.001	-0.511	<0.001	0.369	<0.001	0.364	<0.001

Abbreviations: RA, right atrium; RVFWS, right ventricular free wall strain; RVGLS, right ventricular global longitudinal strain; RV S', systolic excursion velocity; TAPSE, tricuspid annular plane systolic excursion

a strong correlation between  $RAS_r$  and  $RAS_{cd}$  while a very good correlation was seen between  $RAS_r$  and  $RAS_{ct}$ , and a modest correlation was observed between  $RAS_{cd}$  and  $RAS_{ct}$ . There was a moderate correlation between  $RAS_r$  and  $RAS_{cd}$  phases with RV  $S'$ , TAPSE, RVGLS, and RV free wall strain while there was a weak correlation between  $RAS_{ct}$  and the RVGLS, and RV free wall strain.

After recognizing the relationship between notch formation and  $RAS_{ct}$ ,  $RAS_{ct}$  was evaluated to determine a cut-off value as an independent predictor of notch formation by receiver operator characteristic (ROC) analysis. The  $RAS_{ct}$  value of  $-19\%$  was identified as the most accurate predictor for notch formation (Supplementary material, *Figure S1*). The ROC area was 0.897 (95% CI, 0.844–0.951;  $P < 0.001$ ). Sensitivity was calculated as 80% while specificity was 87.3%. Positive and negative predictive values were reported as 75.7%, and 69.1%, respectively.

## DISCUSSION

To the best of our knowledge, this is the first study that has investigated the relationship between the TAPSE curve and speckle-tracking-derived RA strain measurements in all 3 phases, especially with the booster phase  $RAS_{ct}$ .

Our findings can be summarized as follows: (1) the TAPSE curve configuration has a relationship with the RAS parameters; (2) both TAPSE and RAS have similar courses when  $RAS_{ct}$  remains preserved; (3) especially the descending arm of the TAPSE curve holds a clue with respect to  $RAS_{ct}$ ; (4) TAPSE has a notch on the descending arm of its curve if  $RAS_{ct}$  is above  $-19\%$ .

It is well-known that strain is a dimensionless metric of myocardial function and deformation of the myocardium; it is calculated as the percentage of systolic shortening [8, 12]. It has also been established that atrial and ventricular functions are interrelated. When we compare the atrium-to-ventricle strain analyses, atrial strain is thought to be more difficult and time-consuming. The reasons are the far-field location of the atrium, thin atrial walls, the presence of the appendage and veins that drain into the atria, and the need for more focused atrial views [6, 8]. It has been shown that RAS is a cutting-edge technique with great potential in different clinical scenarios and a reliable tool to study RA performance, but it is also methodologically complex and difficult to interpret. RA dysfunction by strain assessments could be demonstrated in several disorders including PH [13, 14], coronary artery disease [15], HF [16], atrial fibrillation, or in top-level athletes [17]. RAS, especially  $RAS_r$ , plays a role as a prognostic indicator for pre-capillary PH [13]; moreover, RA and RV strains detect subclinical changes in RV function in pre-capillary PH as well [10]. In patients with stable coronary artery disease, RAS as a marker for atrial wall deformation occurs early in coronary artery disease, even before any changes in atrial volumes or dimensions [15]. Also, RA function, as assessed by strain imaging, correlates with right heart hemodynamics in patients with heart failure with reduced ejection fraction

(HFrEF) [18]. This imaging tool serves as an invaluable ally for guiding diagnosis, prognosis, and management of HF [19]. There is accumulating evidence that right atrial imaging has a wide range of potential clinical applications. One of the challenges to widespread clinical application of these techniques has been the lack of both standardization of the parameters to be measured and specific software packages to use to obtain such measurements.

On the other hand, TAPSE is the most commonly used echocardiographic tool for evaluation of RV function. Its popularity comes from the ease of its application, it being less dependent on optimal image quality than other measurements, its high reproducibility, and its good correlation with RV stroke volume [20]. We noticed that some patients have a notch in the descending arm in response to the late diastole phase where we expected the atrial contraction contribution while others had a smooth descending arm. Therefore we investigated the utility of TAPSE configuration for estimation of  $RAS_{ct}$  in daily routine. There is a lack of data about configuration differences and determinants of the TAPSE curve thus far. At the end of the recording of all of the RA/ RV strain parameters and TAPSE in the same examination, along with electrocardiography monitoring, the analyses showed that the majority of the study population (71.7%) demonstrated this notch formation. RAS and TAPSE curves showed similar shapes throughout the cardiac cycle while RV strain showed similar yet inverted shapes (*Figure 1*).  $RAS_{ct}$  was lower in the patients without notching on TAPSE, even after taking into consideration lower TAPSE, RV function, and enlarged RV sizes. We assume that the decline in the TAPSE curve, especially the terminal part of this descent corresponding to the late diastole where the P wave occurs, plays a role as an indicator of  $RAS_{ct}$ . It was demonstrated that this hump in the descending arm disappears when the atrial contribution diminishes, and  $RAS_{ct}$  drops below  $-19\%$  (*Figure 3*). We suggest that TAPSE, which is an easily applicable imaging tool, can serve as an invaluable guide to estimate  $RAS_{ct}$ .

Strain analyses of the atrium serve as an indicator of the 3 different phases of atrial functions during the cardiac cycle. The first positive deflection of the strain curve represents the reservoir phase. It occurs when the RV contracts and the RA fills against a closed tricuspid valve. As might be expected, this metric is influenced by long-axis ventricular contraction (higher RVGLS and RV free wall strain bring higher TAPSE values, and accordingly, higher  $RAS_r$  values), RA compliance, and RA volumes [21–23]. Our results demonstrated that  $RAS_r$  showed a higher correlation with RVGLS, RV free wall strain, and TAPSE than the  $RAS_{cd}$  and  $RAS_{ct}$  parameters. The study of Barbier et al. [24] underlined that longitudinal ventricular function is a key determinant of atrial reservoir function. All RAS values were higher for the patients who had notch formation in the TAPSE curve and each of the three tended to be low with tachycardia. This can be explained by the negative impact of tachycardia on atrial functions due to the shorter filling time and,

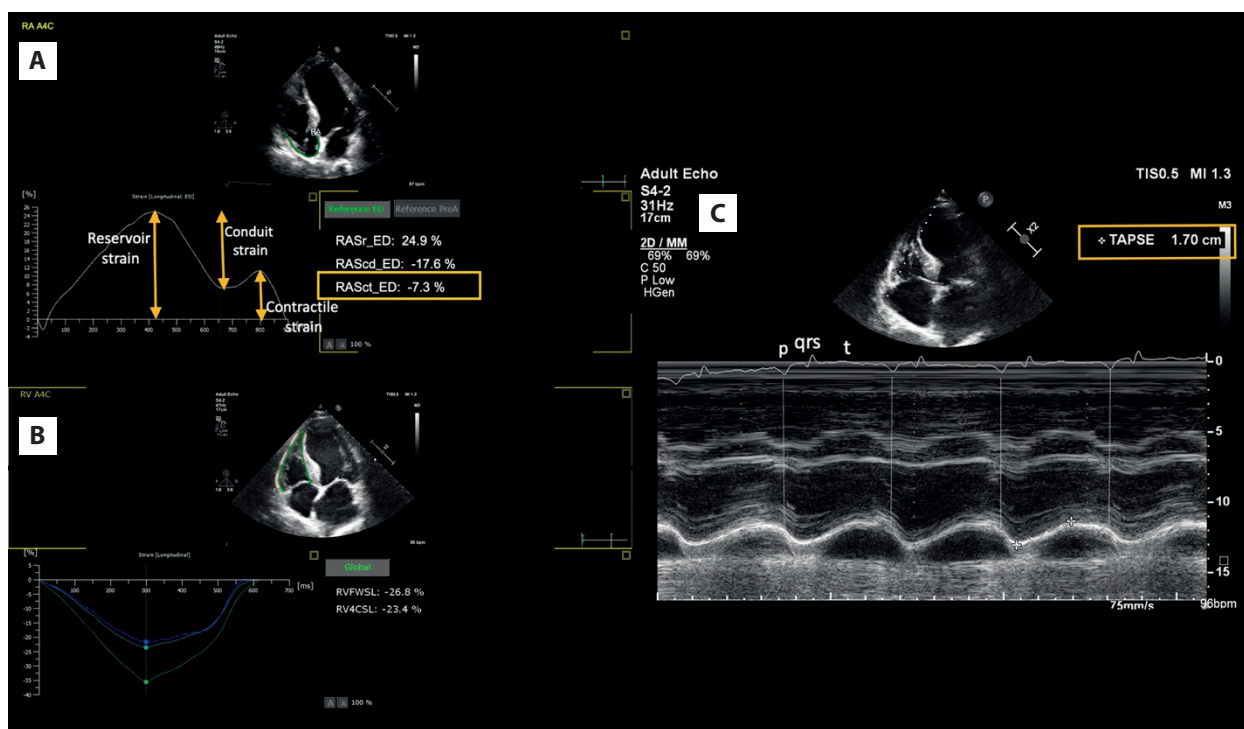


**Figure 3.** Demonstration of lower contractile strain indicates the TAPSE curve without notch formation. **A.** Right atrial strain curve. **B.** Right ventricular strain curves. **C.** TAPSE analyses and a TAPSE curve without notch formation in the descending arm

Abbreviations: RA<sub>s</sub>\_ED, end-diastolic right atrial reservoir strain; RA<sub>cd</sub>\_ED, end-diastolic right atrial conduit strain; RA<sub>ct</sub>\_ED, end-diastolic right atrial contractile strain; RVFWSL, right ventricular free wall strain; RVGLS, right ventricular global longitudinal strain; TAPSE, tricuspid annular plane systolic excursion

consequently, inadequate suction of the ventricles. Some studies have claimed that there is a correlation between the heart rate and aggravation in atrial contraction while other studies have not supported this notion [25, 26]. The general opinion about the effect of tachycardia on diastolic filling is that tachycardia will shorten the E wave deceleration time and fuse the E and A waves, and the mitral A wave will be higher in velocity because of the shortened diastolic filling time [27]. Thus, one might observe a reduction with RA<sub>r</sub> and RA<sub>cd</sub> and an increase with RA<sub>ct</sub>. However, a large-scale meta-analysis of RAS showed that tachycardia did not have the effect of increasing contractile reserve [28]. In our study, we have found a strong relationship between the absence of notch formation on TAPSE and tachycardia (Tables 1, 2).

On the other hand, when the literature was searched for studies about RAS analyses, we observed that most of the previous studies investigated healthy subjects for normal reference ranges of RAS parameters and differences between ages, geography, and sex [20, 29–31]. First, Padeletti et al. [29] reported in 2012 that RA<sub>r</sub> was found at a rate of 49% (13) for 84 healthy individuals [29]. Then in 2013, Peluso et al. [30] expanded the strain investigation with volumetric research and reported strain values in normal ranges in 200 healthy volunteers for 3 different strain values. They reported that RA<sub>r</sub> was found at a rate of 44% (10), while for RA<sub>cd</sub> it was 27% (9), and for RA<sub>ct</sub> it was -17% (4). Afterward in 2018, Brand et al. [31] investigated strain values in 123 women without known cardio-

vascular disease or risk factors. Ultimately, Soulat-Dufour et al. [11] conducted the largest multi-center study with 2008 healthy adults. Both Brand et al. and Soulat-Dufour et al. indicated differences according to sex. Soulat-Dufour et al. reported that RA<sub>r</sub> was found at a rate of 45.8% (13), RA<sub>cd</sub> at -18.4% (7.5), and RA<sub>ct</sub> at -27.6% (9.7). We found similar strain values as the previous studies; they were as follows: RA<sub>r</sub> was 39.5% (13.6), RA<sub>cd</sub> was -18.2% (6.3), and RA<sub>ct</sub> was -21.3% (6.7). The correlation between RA<sub>r</sub> and RA<sub>cd</sub>, RA<sub>r</sub> and RA<sub>ct</sub> was very strong while a modest relationship was observed between RA<sub>cd</sub> and RA<sub>ct</sub> in the current study. In a study by Vijiic et al. [32], the authors investigated RA phasic functions in left-sided heart failure, and they demonstrated that RA<sub>r</sub>, RA<sub>cd</sub>, and RA<sub>ct</sub> are all impaired. They also found similar correlations as ours between RAS and RVGLS. We found that RA<sub>r</sub> showed a negative correlation with RVGLS ( $r = -0.48$ ), and they also demonstrated a negative correlation ( $r = -0.53$ ). The same is true for the correlation between RA<sub>ct</sub> and RVGLS. We found a positive correlation between RA<sub>ct</sub> and RVGLS ( $r = 0.36$ ) in parallel with their findings ( $r = 0.35$ ).

Nevertheless, the interaction between RA<sub>ct</sub> and other echocardiographic parameters, such as the RV S', TAPSE, RVGLS, and RV free wall strain, was less pronounced than the interaction between reservoir and conduit phases. On the other hand, RA<sub>ct</sub> emerged as the predictor of notch formation in the TAPSE curve along with RVGLS and RV free wall strain. Thus, we accept that RA<sub>ct</sub> has the power

to represent the TAPSE curve configuration irrespective of the impact of other echocardiographic parameters.

## CONCLUSION

The changes in the TAPSE curve configuration reflect the changes in the atrial contractile phase. The TAPSE curve has two different configurations, which have a notched or a smooth form. This difference corresponds to late diastole, which represents the atrial contractile phase. The descending arm of the TAPSE curve indicates whether  $RAS_{ct}$  is preserved or not. Notch formation persists if  $RAS_{ct}$  is above  $-19\%$ . Thus, TAPSE, which is an easier and more available tool, can be accepted as an indicator of the atrial contractile phase. We suggest that the TAPSE curve configuration can be used to estimate  $RAS_{ct}$  in daily practice.

## Supplementary material

Supplementary material is available at [https://journals.viamedica.pl/kardiologia\\_polska](https://journals.viamedica.pl/kardiologia_polska)

## Article information

**Conflict of interest:** None declared.

**Funding:** None.

**Open access:** This article is available in open access under Creative Commons Attribution-Non-Commercial-No Derivatives 4.0 International (CC BY-NC-ND 4.0) license, which allows downloading and sharing articles with others as long as they credit the authors and the publisher, but without permission to change them in any way or use them commercially. For commercial use, please contact the journal office at [kardiologiapolska@ptkardio.pl](mailto:kardiologiapolska@ptkardio.pl).

## REFERENCES

- Tadic M. The right atrium, a forgotten cardiac chamber: An updated review of multimodality imaging. *J Clin Ultrasound*. 2015; 43(6): 335–345, doi: [10.1002/jcu.22261](https://doi.org/10.1002/jcu.22261), indexed in Pubmed: [25732678](https://pubmed.ncbi.nlm.nih.gov/25732678/).
- Chow V, Ng AC, Chung T, et al. Right atrial to left atrial area ratio on early echocardiography predicts long-term survival after acute pulmonary embolism. *Cardiovasc Ultrasound*. 2013; 11: 17, doi: [10.1186/1476-7120-11-17](https://doi.org/10.1186/1476-7120-11-17), indexed in Pubmed: [23725312](https://pubmed.ncbi.nlm.nih.gov/23725312/).
- Raymond RJ, Hinderliter AL, Willis PW, et al. Echocardiographic predictors of adverse outcomes in primary pulmonary hypertension. *J Am Coll Cardiol*. 2002; 39(7): 1214–1219, doi: [10.1016/s0735-1097\(02\)01744-8](https://doi.org/10.1016/s0735-1097(02)01744-8), indexed in Pubmed: [11923049](https://pubmed.ncbi.nlm.nih.gov/11923049/).
- Sallach JA, Tang WH, Borowski AG, et al. Right atrial volume index in chronic systolic heart failure and prognosis. *JACC Cardiovasc Imaging*. 2009; 2(5): 527–534, doi: [10.1016/j.jcmg.2009.01.012](https://doi.org/10.1016/j.jcmg.2009.01.012), indexed in Pubmed: [19442936](https://pubmed.ncbi.nlm.nih.gov/19442936/).
- Nemes A, Forster T. [Echocardiographic evaluation of the right atrium - from M-mode to 3D speckle-tracking imaging]. *Orv Hetil*. 2016; 157(43): 1698–1707, doi: [10.1556/650.2016.30546](https://doi.org/10.1556/650.2016.30546), indexed in Pubmed: [27774804](https://pubmed.ncbi.nlm.nih.gov/27774804/).
- Lang RM, Cameli M, Sade LE, et al. Imaging assessment of the right atrium: anatomy and function. *Eur Heart J Cardiovasc Imaging*. 2022; 23(7): 867–884, doi: [10.1093/ehjci/jeac011](https://doi.org/10.1093/ehjci/jeac011), indexed in Pubmed: [35079782](https://pubmed.ncbi.nlm.nih.gov/35079782/).
- Rai AB, Lima E, Munir F, et al. Speckle tracking echocardiography of the right atrium: the neglected chamber. *Clin Cardiol*. 2015; 38(11): 692–697, doi: [10.1002/clc.22438](https://doi.org/10.1002/clc.22438), indexed in Pubmed: [26418622](https://pubmed.ncbi.nlm.nih.gov/26418622/).
- Badano LP, Kolias TJ, Muraru D, et al. Standardization of left atrial, right ventricular, and right atrial deformation imaging using two-dimensional speckle tracking echocardiography: a consensus document of the EACVI/ASE/Industry Task Force to standardize deformation imaging. *Eur Heart J Cardiovasc Imaging*. 2018; 19(6): 591–600, doi: [10.1093/ehj-ci/jeu042](https://doi.org/10.1093/ehj-ci/jeu042), indexed in Pubmed: [29596561](https://pubmed.ncbi.nlm.nih.gov/29596561/).
- Miller D, Farah MG, Liner A, et al. The relation between quantitative right ventricular ejection fraction and indices of tricuspid annular motion and myocardial performance. *J Am Soc Echocardiogr*. 2004; 17(5): 443–447, doi: [10.1016/j.echo.2004.01.010](https://doi.org/10.1016/j.echo.2004.01.010), indexed in Pubmed: [15122184](https://pubmed.ncbi.nlm.nih.gov/15122184/).
- Rudski LG, Lai WW, Afilalo J, et al. Guidelines for the echocardiographic assessment of the right heart in adults: a report from the American Society of Echocardiography endorsed by the European Association of Echocardiography, a registered branch of the European Society of Cardiology, and the Canadian Society of Echocardiography. *J Am Soc Echocardiogr*. 2010; 23(7): 685–713; quiz 786, doi: [10.1016/j.echo.2010.05.010](https://doi.org/10.1016/j.echo.2010.05.010), indexed in Pubmed: [20620859](https://pubmed.ncbi.nlm.nih.gov/20620859/).
- Soulat-Dufour L, Addetia K, Miyoshi T, et al. Normal Values of Right Atrial Size and Function According to Age, Sex, and Ethnicity: Results of the World Alliance Societies of Echocardiography Study. *J Am Soc Echocardiogr*. 2021; 34(3): 286–300, doi: [10.1016/j.echo.2020.11.004](https://doi.org/10.1016/j.echo.2020.11.004), indexed in Pubmed: [33212183](https://pubmed.ncbi.nlm.nih.gov/33212183/).
- Voigt JU, Pedrizzetti G, Lysyansky P, et al. Definitions for a common standard for 2D speckle tracking echocardiography: consensus document of the EACVI/ASE/Industry Task Force to standardize deformation imaging. *Eur Heart J Cardiovasc Imaging*. 2015; 16(1): 1–11, doi: [10.1093/ehj-ci/jeu184](https://doi.org/10.1093/ehj-ci/jeu184), indexed in Pubmed: [25525063](https://pubmed.ncbi.nlm.nih.gov/25525063/).
- Hasselberg NE, Kagiya N, Soyama Y, et al. The prognostic value of right atrial strain imaging in patients with precapillary pulmonary hypertension. *J Am Soc Echocardiogr*. 2021; 34(8): 851–861.e1, doi: [10.1016/j.echo.2021.03.007](https://doi.org/10.1016/j.echo.2021.03.007), indexed in Pubmed: [33774108](https://pubmed.ncbi.nlm.nih.gov/33774108/).
- Vos JL, Leiner T, van Dijk APJ, et al. Right atrial and ventricular strain detects subclinical changes in right ventricular function in precapillary pulmonary hypertension. *Int J Cardiovasc Imaging*. 2022 [Epub ahead of print], doi: [10.1007/s10554-022-02555-6](https://doi.org/10.1007/s10554-022-02555-6), indexed in Pubmed: [35190941](https://pubmed.ncbi.nlm.nih.gov/35190941/).
- Khedr L, Elasar A, Hekal S, et al. Assessment of left and right atrial geometrical changes in patients with stable coronary artery disease: Left and right atrial strain and strain rate imaging study. *Egypt Heart J*. 2018; 70(2): 101–106, doi: [10.1016/j.ehj.2018.02.003](https://doi.org/10.1016/j.ehj.2018.02.003), indexed in Pubmed: [30166890](https://pubmed.ncbi.nlm.nih.gov/30166890/).
- Vakilian F, Tavallaie A, Alimi H, et al. Right atrial strain in the assessment of right heart mechanics in patients with heart failure with reduced ejection fraction. *J Cardiovasc Imaging*. 2021; 29(2): 135–143, doi: [10.4250/jcvi.2020.0092](https://doi.org/10.4250/jcvi.2020.0092), indexed in Pubmed: [33605100](https://pubmed.ncbi.nlm.nih.gov/33605100/).
- D'Ascenzi F, Cameli M, Padeletti M, et al. Characterization of right atrial function and dimension in top-level athletes: a speckle tracking study. *Int J Cardiovasc Imaging*. 2013; 29(1): 87–94, doi: [10.1007/s10554-012-0063-z](https://doi.org/10.1007/s10554-012-0063-z), indexed in Pubmed: [22588713](https://pubmed.ncbi.nlm.nih.gov/22588713/).
- Olsen FJ, Biering-Sørensen T. Right atrial strain: Tapping into a new reservoir of hemodynamic information. *Int J Cardiol*. 2021; 326: 226–228, doi: [10.1016/j.ijcard.2020.11.009](https://doi.org/10.1016/j.ijcard.2020.11.009), indexed in Pubmed: [33217481](https://pubmed.ncbi.nlm.nih.gov/33217481/).
- Ponikowski P, Voors AA, Anker SD, et al. 2016 ESC Guidelines for the diagnosis and treatment of acute and chronic heart failure: The Task Force for the diagnosis and treatment of acute and chronic heart failure of the European Society of Cardiology (ESC) Developed with the special contribution of the Heart Failure Association (HFA) of the ESC. *Eur Heart J*. 2016; 37(27): 2129–2200, doi: [10.1093/eurheartj/ehw128](https://doi.org/10.1093/eurheartj/ehw128), indexed in Pubmed: [27206819](https://pubmed.ncbi.nlm.nih.gov/27206819/).
- Hu R, Mazer CD, Tousignant C. Relationship between tricuspid annular excursion and velocity in cardiac surgical patients. *J Cardiothorac Vasc Anesth*. 2014; 28(5): 1198–1202, doi: [10.1053/j.jvca.2013.10.005](https://doi.org/10.1053/j.jvca.2013.10.005), indexed in Pubmed: [24447502](https://pubmed.ncbi.nlm.nih.gov/24447502/).
- Addetia K, Takeuchi M, Maffessanti F, et al. Simultaneous longitudinal strain in all 4 cardiac chambers: a novel method for comprehensive functional assessment of the heart. *Circ Cardiovasc Imaging*. 2016; 9(3): e003895, doi: [10.1161/CIRCIMAGING.115.003895](https://doi.org/10.1161/CIRCIMAGING.115.003895), indexed in Pubmed: [26926268](https://pubmed.ncbi.nlm.nih.gov/26926268/).
- Solomon SD, Biering-Sørensen T. LA strain when ejection fraction is preserved: a new measure of diastolic function? *JACC Cardiovasc Imaging*. 2017; 10(7): 744–746, doi: [10.1016/j.jcmg.2016.09.018](https://doi.org/10.1016/j.jcmg.2016.09.018), indexed in Pubmed: [28017382](https://pubmed.ncbi.nlm.nih.gov/28017382/).
- Ersbøll M, Andersen MJ, Valeur N, et al. The prognostic value of left atrial peak reservoir strain in acute myocardial infarction is dependent on left ventricular longitudinal function and left atrial size. *Circ Cardiovasc Im-*

- aging. 2013;6(1):26–33, doi: [10.1161/CIRCIMAGING.112.978296](https://doi.org/10.1161/CIRCIMAGING.112.978296), indexed in Pubmed: [23192848](https://pubmed.ncbi.nlm.nih.gov/23192848/).
24. Barbier P, Solomon S, Schiller N, et al. Left atrial relaxation and left ventricular systolic function determine left atrial reservoir function. *Circulation*. 1999; 100(4): 427–436, doi: [10.1161/01.cir.100.4.427](https://doi.org/10.1161/01.cir.100.4.427).
  25. Truong VT, Palmer C, Young M, et al. Right atrial deformation using cardiovascular magnetic resonance myocardial feature tracking compared with two-dimensional speckle tracking echocardiography in healthy volunteers. *Sci Rep*. 2020; 10(1): 5237, doi: [10.1038/s41598-020-62105-9](https://doi.org/10.1038/s41598-020-62105-9), indexed in Pubmed: [32251322](https://pubmed.ncbi.nlm.nih.gov/32251322/).
  26. Qu YY, Buckert D, Ma GS, et al. Quantitative assessment of left and right atrial strains using cardiovascular magnetic resonance based tissue tracking. *Front Cardiovasc Med*. 2021; 8: 690240, doi: [10.3389/fcvm.2021.690240](https://doi.org/10.3389/fcvm.2021.690240), indexed in Pubmed: [34250043](https://pubmed.ncbi.nlm.nih.gov/34250043/).
  27. Bierig S, Hill J. Echocardiographic evaluation of diastolic function. *Journal of Diagnostic Medical Sonography*. 2011; 27(2): 65–78, doi: [10.1177/8756479311401914](https://doi.org/10.1177/8756479311401914).
  28. Pathan F, D'Elia N, Nolan MT, et al. Normal ranges of left atrial strain by speckle-tracking echocardiography: a systematic review and meta-analysis. *J Am Soc Echocardiogr*. 2017; 30(1): 59–70.e8, doi: [10.1016/j.echo.2016.09.007](https://doi.org/10.1016/j.echo.2016.09.007), indexed in Pubmed: [28341032](https://pubmed.ncbi.nlm.nih.gov/28341032/).
  29. Padeletti M, Cameli M, Lisi M, et al. Reference values of right atrial longitudinal strain imaging by two-dimensional speckle tracking. *Echocardiography*. 2012; 29(2): 147–152, doi: [10.1111/j.1540-8175.2011.01564.x](https://doi.org/10.1111/j.1540-8175.2011.01564.x), indexed in Pubmed: [22118219](https://pubmed.ncbi.nlm.nih.gov/22118219/).
  30. Peluso D, Badano LP, Muraru D, et al. Right atrial size and function assessed with three-dimensional and speckle-tracking echocardiography in 200 healthy volunteers. *Eur Heart J Cardiovasc Imaging*. 2013; 14(11): 1106–1114, doi: [10.1093/ehjci/jet024](https://doi.org/10.1093/ehjci/jet024), indexed in Pubmed: [23423966](https://pubmed.ncbi.nlm.nih.gov/23423966/).
  31. Brand A, Bathe M, Hübscher A, et al. Normative reference data, determinants, and clinical implications of right atrial reservoir function in women assessed by 2D speckle-tracking echocardiography. *Echocardiography*. 2018; 35(10): 1542–1549, doi: [10.1111/echo.14092](https://doi.org/10.1111/echo.14092), indexed in Pubmed: [29962056](https://pubmed.ncbi.nlm.nih.gov/29962056/).
  32. Vijiic A, Vătăşescu R, Onciul S, et al. Right atrial phasic function and outcome in patients with heart failure and reduced ejection fraction: Insights from speckle-tracking and three-dimensional echocardiography. *Kardiol Pol*. 2022; 80(3): 322–331, doi: [10.33963/KP.a2022.0044](https://doi.org/10.33963/KP.a2022.0044), indexed in Pubmed: [35152396](https://pubmed.ncbi.nlm.nih.gov/35152396/).